Analytical and Bioanalytical Chemistry (2024) 416:4727–4737
https://doi.org/10.1007/s00216-024-05437-z

PAPER IN FOREFRONT

Real-time monitoring of cellular superoxide anion release in THP-1 cells using a catalytically amplified superoxide dismutase–based microbiosensor

Aaditya S. Deshpande[1] · Tyler Bechard[1] · Emily DeVoe[1] · Jared Morse[1] · Reem Khan[1] · Ka Ho Leung[1] · Silvana Andreescu[1,2]

Received: 7 June 2024 / Revised: 1 July 2024 / Accepted: 2 July 2024 / Published online: 17 July 2024

Abstract

Reactive oxygen species (ROS) including the superoxide anion ($O_2^{\bullet-}$) are typically studied in cell cultures using fluorescent dyes, which provide only discrete single-point measurements. These methods lack the capabilities for assessing $O_2^{\bullet-}$ kinetics and release in a quantitative manner over long monitoring times. Herein, we present the fabrication and application of an electrochemical biosensor that enables real-time continuous monitoring of $O_2^{\bullet-}$ release in cell cultures for extended periods (> 8 h) using an $O_2^{\bullet-}$ specific microelectrode. To achieve the sensitivity and selectivity requirements for cellular sensing, we developed a biohybrid system consisting of superoxide dismutase (SOD) and $Ti_3C_2T_x$ MXenes, deposited on a gold microwire electrode (AuME) as $O_2^{\bullet-}$ specific materials with catalytic amplification through the synergistic action of the enzyme and the biomimetic MXenes-based structure. The biosensor demonstrated a sensitivity of 18.35 nA/μM with a linear range from 147 to 930 nM in a cell culture medium. To demonstrate its robustness and practicality, we applied the biosensor to monitor $O_2^{\bullet-}$ levels in human leukemia monocytic THP-1 cells upon stimulation with lipopolysaccharide (LPS). Using this strategy, we successfully monitored LPS-induced $O_2^{\bullet-}$ in THP-1 cells, as well as the quenching effect induced by the ROS scavenger N-acetyl-L-cysteine (NAC). The biosensor is generally useful for exploring the role of oxidative stress and longitudinally monitoring $O_2^{\bullet-}$ release in cell cultures, enabling studies of biochemical processes and associated oxidative stress mechanisms in cellular and other biological environments.

Keywords Superoxide anion · Biosensor · Real-time monitoring · Cell culture · Oxidative stress

Introduction

Reactive oxygen species, or ROS, involve small reactive molecules such as superoxide ($O_2^{\bullet-}$), hydrogen peroxide (H_2O_2), and the hydroxyl radical ($^{\bullet}OH$) that are short-lived and thus difficult to measure. $O_2^{\bullet-}$ measurement is of great importance due to its involvement in the onset of several pathologies and disease conditions. The damage to proteins and genes caused by the overproduction of ROS has been linked with the onset of cancer [1], Alzheimer's and Parkinson's diseases, among others [2]. ROS species are formed primarily due to the spin restriction present on triplet molecular oxygen [3]. In biological systems, the single electron reduction of molecular oxygen occurs as a byproduct of several organelle reactions, with the cellular respiration performed by mitochondria causing $O_2^{\bullet-}$ in most organisms. The generation of $O_2^{\bullet-}$ is controlled through an extensive network of antioxidant molecules that limit the overproduction of ROS and ensure normal homeostatic function. Under normal conditions, ROS plays an important role in signaling cell behavior and defense mechanisms [4]. However, when the concentration of ROS exceeds a level that cannot be offset by the antioxidants present in the system, oxidative stress

Published in the topical collection *Emerging Trends in Electrochemical Analysis* with guest editors Sabine Szunerits, Wei Wang, and Adam T. Woolley.

✉ Silvana Andreescu
eandrees@clarkson.edu

[1] Department of Chemistry and Biomolecular Science, Clarkson University, 8 Clarkson Avenue, Potsdam, NY 13699-5810, USA

[2] Department of Environmental Health Sciences, Robert Stempel College of Public Health, Florida International University (FIU), 11200 SW 8th Street, AHC-5, Miami, FL 33199, USA

occurs. This can induce damage to proteins, DNA, and cells, including peroxidation of lipid membranes, carbonylation of proteins, and DNA damage, leading to the development of diseases. Measurement of ROS is important for understanding the oxidant-antioxidant balance and studying conditions involved in the onset and progression of diseases.

Conventional methods to quantify $O_2^{\bullet-}$ are limited by long assay times and lack of capabilities for measuring release of these species in situ, providing only discrete endpoint information on collected samples. Current methods include electron paramagnetic resonance and photon emission spectroscopy [5–7], fluorescence spectroscopy with ROS/RNS-specific dyes [8], ultraviolet–visible spectrophotometry [9], and chemiluminescence [10]. Quantification of ROS in cell cultures is typically carried out by fluorescence spectroscopy with ROS-specific dyes. Electrochemical biosensors are a viable alternative to these conventional assays, offering the advantage of a single-step measurement that can be conducted with the electrochemical probe inserted in cell cultures, thus providing real-time monitoring of the evolution and kinetics of $O_2^{\bullet-}$ [11, 12]. To develop an effective electrochemical probe for $O_2^{\bullet-}$, considerable efforts have focused on the discovery of new electrode materials and compositions to selectively react with $O_2^{\bullet-}$, typically with the help of biological or biomimetic catalysts, facilitating a directly quantifiable measure of ROS in the biological environment. Examples of electrode modification include the use of cytochrome *c* (Cyt C) immobilized onto the surface of gold microwires, generating a current proportional to the $O_2^{\bullet-}$ concentration [13–15]. Superoxide dismutase (SOD) has been used as an alternative biological catalyst, which allows the specific disproportionation of $O_2^{\bullet-}$ to O_2 and H_2O_2 [16, 17] which can be assayed and used to estimate the amount and rate of $O_2^{\bullet-}$ production. SOD are ubiquitous metalloproteins in oxygen-tolerant organisms protecting against oxidative damage caused by ROS [18]. They contain a metal ion cofactor and include copper/zinc-containing SOD (Cu/Zn-SOD), manganese-containing SOD (Mn-SOD), iron-containing SOD (Fe-SOD), and nickel-containing SOD (Ni-SOD) [19–21]. The Cu/Zn-SOD has been widely used in electrochemical biosensors due to the more efficient electron transfer [22–26]. In a typical design, SOD is immobilized on an electrode surface to catalyze the dismutation of the $O_2^{\bullet-}$ to O_2 and H_2O_2, via a two-step process in which the metal ion (e.g., copper) of the metalloprotein switches between copper(I) and copper(II) for example, as follows:

$$O_2^{-} + \text{Cu(II)ZnSOD} \rightarrow O_2 + \text{Cu(I)ZnSOD} \quad (1)$$

$$O_2^{-} + \text{Cu(I)ZnSOD} + 2H^{+} \rightarrow H_2O_2 + \text{Cu(II)ZnSOD} \quad (2)$$

$$\text{Overall reaction stoichiometry is}: 2O_2^{-} + 2H^{+} \rightarrow H_2O_2 + O_2 \quad (3)$$

The enzymatically produced H_2O_2 is detected at the characteristic potential corresponding to the oxido-reduction of H_2O_2. One limitation of this design is that the applied potential for the oxidation of H_2O_2 is typically high (> 0.5 V vs Ag/AgCl), which can cause interferences from electroactive substances such as ascorbic acid and uric acid that are typically present in biological samples [12]. Moreover, while many studies demonstrate electrochemical measurements of $O_2^{\bullet-}$, in most cases, the sensors are built on micro-size electrodes such as glassy carbon electrodes (GCE) which have restricted usability in small volumes for cell culture work. Strategies to improve selectivity, reduce electrode size, and decrease the potential window outside of the range of interferences are therefore needed to develop biosensors that can efficiently measure $O_2^{\bullet-}$ in cellular systems.

To meet the requirements for measurements in cell cultures on microelectrode probes, it is essential to design suitable electrode materials that can sensitively and specifically detect $O_2^{\bullet-}$ and facilitate real-time monitoring of $O_2^{\bullet-}$ kinetics while maintaining functionality in the culture media and minimizing nonspecific adsorption. In this study, we describe an electrochemical microbiosensor based on SOD with catalytic amplification for the detection of $O_2^{\bullet-}$ in human cells, focusing on leukemia monocyte THP-1 cells. We selected SOD because of its high specificity and fast reaction rate with $O_2^{\bullet-}$.

A general strategy to increase the signal intensity is to use two-dimensional metal carbides [27] which provide high surface area with rich functionalities enabling applications in fields like electrochemical sensing, energy storage/batteries [28], and semiconductors [29]. This unique layered structure and composition, high surface area, conductivity, hydrophilicity, and biocompatibility make MXenes an attractive material for electrochemical biosensors and enzyme immobilization [30]. We interfaced the SOD with two-dimensional layered $Ti_3C_2T_x$ MXenes. We selected $Ti_3C_2T_x$ transition metal carbide (where T_x denotes surface terminations, i.e., oxygen, nitrogen, fluorine, chlorine, hydroxyl) as an electrocatalytic amplifier for H_2O_2 reduction because this material is known to increase efficiency, decrease the measurement potential, and more selectively measure the SOD-generated H_2O_2 [31, 32]. Moreover, the fabrication of $Ti_3C_2T_x$ by chemical etching leads to a series of tightly packed layers with terminal groups that provide anchoring points for biomolecules, increasing bioactivity on microelectrode platforms. A recent example demonstrates the effectiveness of hemoglobin immobilization in MXenes as a detection platform for H_2O_2 measurement [31]. Lorencova et al. have demonstrated that $Ti_3C_2T_x$ MXenes are an excellent electrocatalyst, enabling rapid and ultrasensitive

detection of H_2O_2 down to the nM level [32]. Therefore, we expect that the combined use of SOD with $Ti_3C_2T_x$ MXenes will increase the microelectrode surface area and efficiency of electrode transfer, and thus more selectively measure the SOD-generated H_2O_2 reduction, and thus of $O_2^{\bullet-}$ in cell culture environments. We examined various deposition conditions on a gold microwire electrode (AuME) and established the synergistic effect between SOD and $Ti_3C_2T_x$ MXenes as a biosensor for $O_2^{\bullet-}$.

This novel biosensor is a promising tool for achieving ultrasensitive and selective detection of ROS in mammalian cell cultures. To demonstrate the robustness and practicality of this design, we apply this biosensor to monitor the change of $O_2^{\bullet-}$ level of human leukemia monocyte THP-1 cells upon stimulation of lipopolysaccharide (LPS). We successfully monitored the LPS-induced superoxide in THP-1 cells, which were quenched by the pretreatment of ROS scavenger, N-acetyl-L-cysteine (NAC). To our knowledge, this study presents the first example of electrochemical techniques to measure the changes induced by LPS and NAC on cell lines. Results of this study confirm the advantage of using combined biological and inorganic catalysts for increasing detection sensitivity and selectivity of microbiosensors for ROS measurements in biological environments.

Experimental methods

Materials and reagents

Gold wires were obtained from World Precision Instruments and liquid tape as manufactured by Gardner Bender was purchased from Lowes. Potassium hydroxide was obtained from Fisher Scientific and hydrogen peroxide was acquired from J.T. Baker. N-Hydroxysuccinimide (NHS) was obtained from Fluka and TCI. 1-Ethyl-3-(3-dimethylaminopropyl) carbodiimide hydrochloric acid (EDC) was purchased from AK Scientific. SOD from bovine kidney was bought from Calzyme. L-Cysteine, ascorbic acid (AA), uric acid (UA), 3,4-dihydroxyphenyl acetic acid (DOPAC), Nafion, hypoxanthine, and xanthine oxidase from bovine milk were all acquired from Sigma-Aldrich. Sodium phosphate dibasic was obtained from AK Scientific and potassium phosphate monobasic was purchased from Sigma-Aldrich. Sodium potassium phosphate buffer (PBS) at a concentration of 0.1 M was prepared at different pH values by mixing potassium phosphate monobasic and sodium phosphate dibasic. $Ti_2C_3T_x$ MXenes were synthesized according to established procedures [33] with the MAX phase sources from Nanoshel LLC. N-Acetyl-L-cysteine (NAC) was acquired from Fisher Scientific (PA, USA) and lipopolysaccharides (PLS) from *Escherichia coli* O111:B4 were purchased from Sigma-Aldrich (MO, USA). THP-1 cells were purchased from ATCC (Manassas, VA).

Cell culture methods and maintenance

Cells were cultured in RPMI 1640 medium containing 10% heat-inactivated fetal bovine serum, 10 mM N-2-hydroxyethylpiperazine-N-2-ethane sulfonic acid (HEPES) buffer, 4500 mg/L glucose, 1500 mg/L sodium bicarbonate, 1 nM sodium pyruvate, 100 mg/mL streptomycin, and 100 U/mL penicillin. The cells were maintained at 37 °C and 5% carbon dioxide. All cell culture reagents were purchased from Fisher Scientific (PA, USA) unless otherwise stated.

Instrumentation

In vitro electrochemical experimentation was conducted with the use of a CH1030A electrochemical analyzer manufactured by CH instruments. Cell culture measurements were alternatively conducted with a CH1232B portable bipotentiostat from CH instruments. Experimental techniques, i.e., cyclic voltammetry (CV), amperometry, and differential pulse voltammetry, were performed using a standard three-electrode system. A silver-silver chloride electrode (1M KCl, CHI Instruments, Inc.) was used as the reference electrode, a platinum electrode served as the counter electrode, and a modified gold wire electrode with a tip diameter of 0.5 mm and an exposed length of 10 mm served as the working electrode. All steps requiring incubation were performed in a Boekel Instruments incubator set to 30 °C unless stated otherwise.

Statistical analysis

All measurements were performed in replicates using at least three independently prepared electrodes, and results are reported as mean average (± standard deviation).

Biosensor fabrication

The gold wire electrodes were first cleaned via submersion in piranha solution for a period of half an hour. Electrochemical cleaning was then performed via cycling in the potential range 0–1.5 V in 0.5 M sulfuric acid. The electrode surface was checked for the typical characteristics of a gold electrode. If the procedure was completed and the final cycle does not reflect the characteristic CV of gold, further cleaning was conducted via boiling in around 3 M aqueous potassium hydroxide for a period of half an hour before electrochemical cleaning is repeated. Cleaned electrodes were incubated in aqueous L-cysteine solution at a concentration of 10 mM for a period of 15 min and rinsed with deionized water upon completion. This cysteine-modified

AuME was then incubated in a solution of 200 µM EDC and 50 µM NHS in 6.5 pH PBS buffer for half an hour. Rinsing with deionized water was then repeated before incubation in a 160 µM solution of SOD in 7.5 pH PBS buffer for a period of 1 h. The electrodes were immersed in an aqueous suspension of 5 mg mL^{-1} of $Ti_3C_2T_x$ MXene containing 2.4% wt Nafion for 1 min before undergoing drying at 40 °C for a period of 1 h. Electrochemical pretreatment was then performed in 7.5 pH PBS with differential pulse voltammetry with a 4-mV potential increment, 50-mV pulse amplitude, 50-ms pulse width, 500-ms pulse period from − 0.5 to 0 V for five runs. In the early stages of the procedural development, CVs in 7.5 pH PBS from − 0.5 to 0.5 V at a scan rate of 100 mV/s were collected after every step to verify successful immobilization of SOD. Fabricated electrodes were stored in 0.1 M 7.5 pH PBS until use.

Measurements

Amperometric measurements were conducted in a conventional electrochemical cell in 0.1 M 7.5 pH PBS buffer or cell culture medium with constant stirring. A potential of − 0.2 V was applied throughout all measurements. All measurements were performed at room temperature. Superoxide was generated enzymatically for signal calibration with the addition of concentrations of xanthine oxidase from 0.1 to 80 mU to a solution containing hypoxanthine in a concentration of 100 µM, as reported [13].

Measurement of LPS-induced cellular superoxide

Cells of the THP-1 line were seeded in a quantity of roughly 2×10^6 in 2 mL of complete RPMI medium in a 12-well dish. After treatment with 1 µg/mL of LPS, a fabricated sensor was added to the medium along with a platinum wire counter electrode and silver-silver chloride reference electrode. An amperogram was then collected at a potential of − 0.2 V over a period of hours as the cells are incubated at 37 °C and 5% carbon dioxide. A parallel control experiment was additionally performed without the addition of LPS.

Results and discussion

Microelectrode fabrication

The functional and structural properties of the modified bioelectrodes were first established by CV and scanning electron microscopy (SEM) to demonstrate changes in the electrode surface after co-immobilization of SOD and $Ti_3C_2T_x$ MXene. Nafion was used as a linker to deposit the MXene on the AuME electrode due to its good film-forming behavior, electrical conductivity, and impermeability to negatively charged proteins and interfering species such as ascorbic acid [34, 35]. Nafion ensures a thin evenly coated layer onto the Au microwire electrode and enhances selectivity against cationic molecules. Moreover, since Nafion is a fluoropolymer, it is expected that it will facilitate stabilization of the MXene on the electrode surface through F-F interactions between the F functionalities of the Nafion and those of the Max phase resulting from the HF etching. The AuME was first modified with L-cysteine to provide $–NH_2$ amino groups for anchoring the SOD enzyme through amine bond formation allowing for efficient conjugation of the enzyme. The biosensor fabrication steps are summarized in Fig. 1. Upon fabrication, the biosensor is first calibrated using enzymatically produced $O_2^{\bullet -}$, generated in the reaction of xanthine oxidase (XOD)

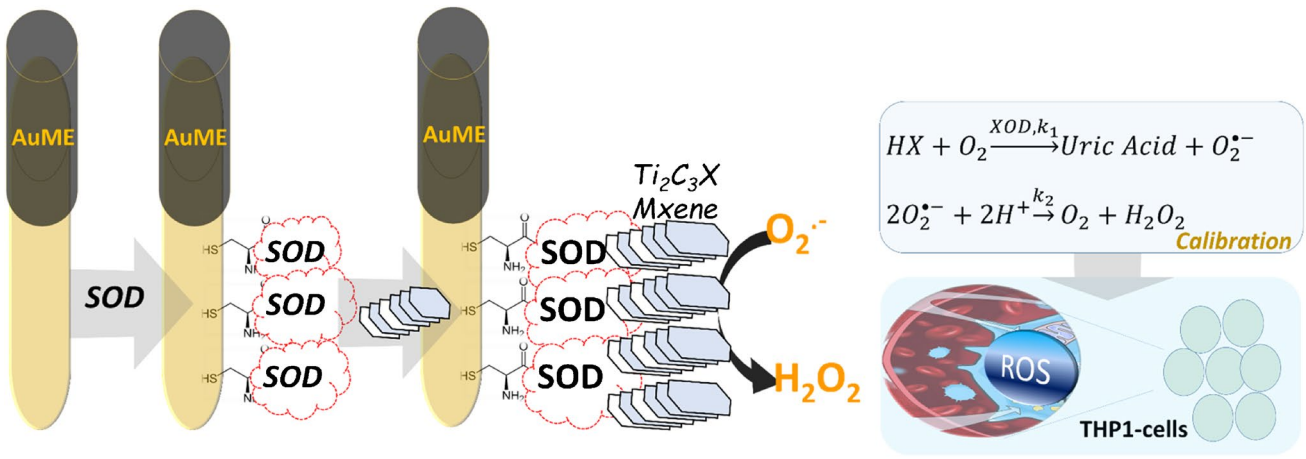

Fig. 1 Fabrication of the SOD-MX-based AuME for $O_2^{\bullet -}$ measurements from enzymatically generated XOD/HX to calibrate the biosensor before being used to quantitatively measure $O_2^{\bullet -}$ release in THP-1 cells. AuME, gold microelectrode; SOD, superoxide dismutase; $Ti_2C_3T_x$, MXenes. The reactions describe the enzymatic generation of $O_2^{\bullet -}$ used to calibrate the sensor

and its substrate, hypoxanthine (HX), which provides a measure of the theoretical $O_2^{\bullet-}$ concentration, before being used to quantify $O_2^{\bullet-}$ in THP-1 cells. Electrochemical measurements of $O_2^{\bullet-}$ are based on the redox reaction involving the electron transfer of the immobilized SOD at the cysteine-modified AuME through the catalytic action of reduced and oxidized SOD through the copper complex moiety that promotes electrode transfer both anodically and cathodically at approximately − 0.2 V/ + 0.2 V vs AgAgCl reference electrode [36]. This approach enables specific measurements of $O_2^{\bullet-}$ without interferences from electroactive molecules that can be found in biological environments including H_2O_2, uric acid, and ascorbic acid.

Studies of electrode morphology, surface modification, and effects on redox processes

The morphology of the $Ti_3C_2T_x$ MXenes studied by SEM is shown in Fig. 2. The as-synthesized $Ti_3C_2T_x$ MXene presents the characteristic two-dimensional multilayered structure upon HF etching. This large surface area arrangement provides rich surface functionalities and sites for catalyzing H_2O_2 decomposition, enhancing $O_2^{\bullet-}$ detection sensitivity. SEM images (Fig. 2B–D) of the surface of the electrode at different stages of fabrication steps show clear changes in the electrode morphology at each modification step. The bare cleaned electrode demonstrates nano-islands of gold in the SEM images, which, after modification with cysteine-SOD appear covered with a smooth uniform layer (Fig. 2B–D). After modification with MXene, novel structures can be observed that lack the distinctive etched surface of MXenes, due to entrapment within Nafion (Fig. 2D).

CVs recorded with the SOD-modified electrode from − 0.5 to + 0.5 V in 0.1 M 7.5 pH PBS at varying scan rates (100 mV/s to 200 mV/s) indicate the presence of the oxidation and reduction peaks at − 0.1 and + 0.1 V, with peak heights linearly correlating with the scan rate (Fig. 3A, B). These features demonstrate a surface confined redox process corresponding to SOD immobilized through the cysteine layer, confirming the success of the enzyme immobilization. Peak height decreased slightly after modification with $Ti_3C_2T_x$ MXenes, likely due to the Nafion layer deposition. It is worth noting that significant instability was exhibited by the sensor without Nafion due to leaching of the MXene from the electrode surface. In the next set of experiments, we studied the electrochemical behavior of the $Ti_3C_2T_x$ MXenes as an electrocatalyst for H_2O_2 oxidation/reduction to establish its potential as a peroxidase mimetic for signal amplification of H_2O_2 detection for the SOD biosensor. Figure 3C shows CVs in the presence and absence of H_2O_2 at the AuME and AuME-MXene-modified electrodes, with a slightly reduced current for the electrode coated with MXene. In the absence of H_2O_2, the CVs show oxidation and reduction peaks typical to an Au electrode surface. In the presence of H_2O_2, the CV of the AuME-MXene shows a significant increase in the oxidation potential starting from around 0.3 V suggesting a catalytic effect towards H_2O_2 oxidation. Within the potential

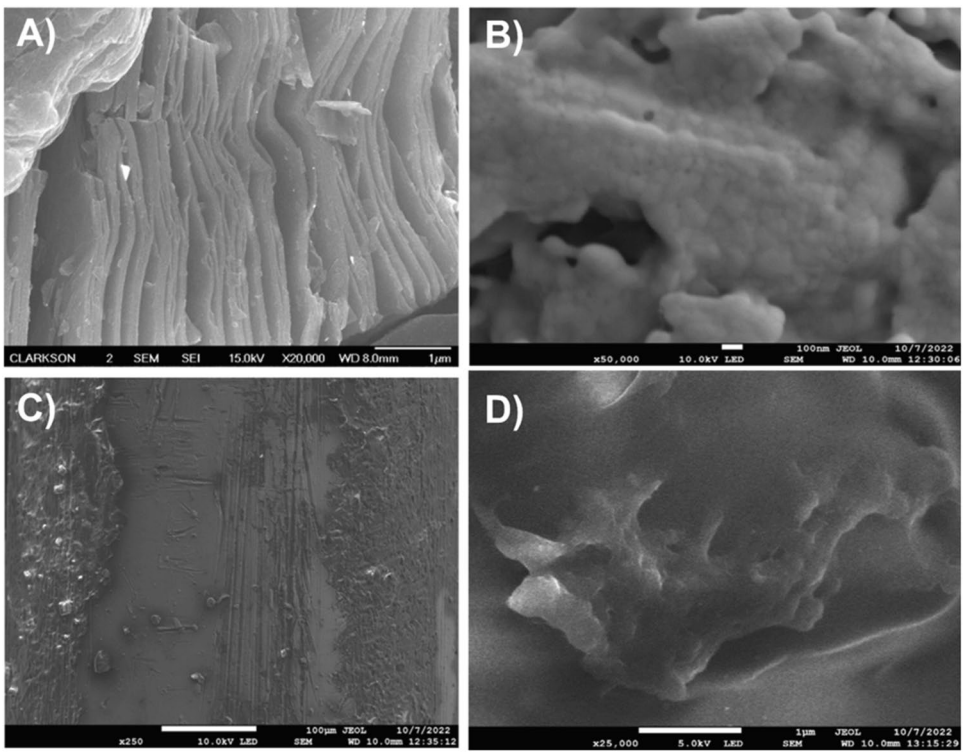

Fig. 2 SEM images of MXene (**A**), sensor surface after cleaning (**B**), sensor surface after superoxide dismutase immobilization step (**C**), and sensor surface after MXene deposition step (**D**). Scale bar: **A**, 1 μm; **B**, 100 nm; **C**, 100 μm; and **D**, 1 μm

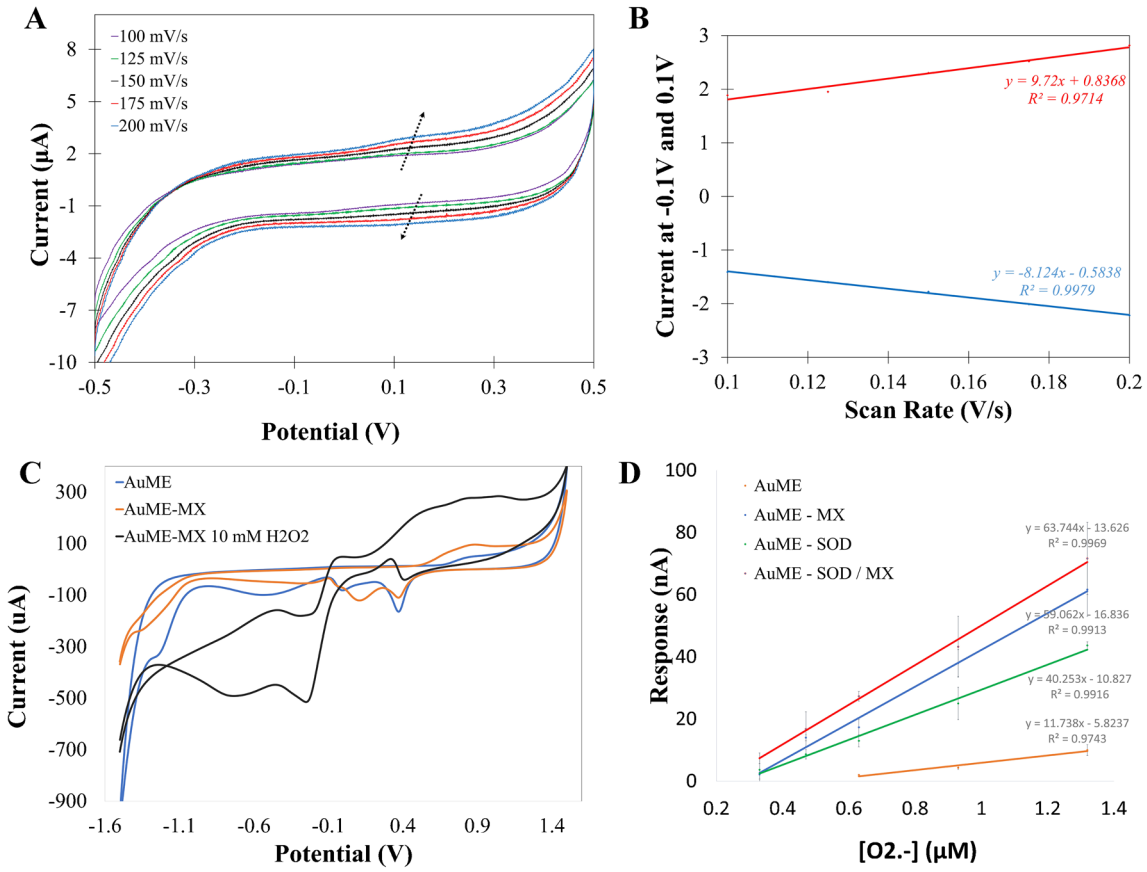

Fig. 3 CVs of the SOD-AuME recorded 0.1 M PBS at various scan rates (**A**). The anodic (blue) and cathodic (red) peak current values plotted against different scan rates (**B**); CVs of bare AuME and modified AuME-MX in absence and presence of H_2O_2 (10 mM) (**C**). Calibration curves for control (bare AuME) and AuME codified with MXene, SOD, and SOD/MXene ($n = 3$) (**D**). All measurements were performed in 0.1 M PBS, pH 7.5, and potential is versus Ag/AgCl (1 M)

range (− 1.5 to 1.5 V vs Ag/AgCl), a large reduction wave with a strong peak at − 0.20 V, corresponding to H_2O_2 reduction was observed. This increase was not noticeable for bare AuME. Similar effects for H_2O_2 reduction have been reported with $Ti_3C_2T_x$ on GCE electrodes [37] which enabled the electroanalytical determination of H_2O_2. CVs recorded in H_2O_2 after each modification steps are summarized in Figure S1, indicating clear changes in the oxidation/reduction peaks after each step, and a significant enhancement being observed for the AuME coated with MXene, confirming a catalytic enhancement effect.

Following confirmation of the electrode modification, we next evaluated the contribution of each electrode coating on the detection of $O_2^{\bullet-}$ after each modification step using HX/XOD to enzymatically generate $O_2^{\bullet-}$ (Fig. 1). To establish the synergistic effect of the MXene and SOD, we first determined the sensitivity of the AuME functionalized with MXene and SOD individually and then in mixture. As can be seen in Fig. 3D, the bare AuME shows extremely small responses to $O_2^{\bullet-}$ which can be due to a small amount of disproportionation to H_2O_2 occurring in the reaction cell. Modification of the AuME with SOD demonstrates quantifiable responses with a sensitivity of 40.25 nA/µM, while coating with MXene alone displayed a sensitivity of 59.06 nA/µM, providing evidence to support the catalytic enhancement. When both MXene and SOD were used, the biosensor displayed the highest sensitivity of 63.74 nA/µM, confirming the enhanced response provided by the combined use of biological and enzyme mimetic catalyst. The control electrode with just cysteine showed current change indistinguishable from background noise at low concentrations of $O_2^{\bullet-}$ and only slight current changes at high concentrations of superoxide. This is likely due to some superoxide undergoing reduction directly at the gold electrode surface due to gaps in the cysteine monolayer.

Biosensor calibration in buffer and cell culture media: analytical performance, reproducibility, and specificity measurements

Analytical performance of the biosensor was established in both buffer and cell culture media by calibration via

succesive additions of XOD to a solution of 0.1 M 7.5 pH PBS containing 100 µM HX, the curves for which are shown in Fig. 4A, B. This enzymatic reaction produces $O_2^{\bullet-}$ and uric acid [15]. The $O_2^{\bullet-}$ ion generated undergoes reduction to form H_2O_2 by the copper center of SOD which is regenerated at − 0.2 V [36]. This low applied potential removes signal from most interfering substances including ascorbic acid and uric acid, which are not oxidized in this potential range. The sensor displayed good linearity from theoretical concentrations of 150 to 1000 nM of $O_2^{\bullet-}$. Calibration of the SOD-MXene AuME under the same conditions was performed in the cell culture medium (RPMI 1640) that was used for measurements in the THP-1 cell line. In both cases, the sensor response reached a steady-state current and stabilized within 1–2 s after addition of HX, after which a stable current was achieved (Fig. 4C). The biosensor gave the sensitivity of 85.15 nA/µM in PBS and 18.35 nA/µM in cell culture medium, while maintaining linearity in both conditions. Reduction in sensitivity in cell culture medium can be attributed to the complex constituent mixture and the lower conductivity of the cell culture medium, with possible attachment of proteins and other charged molecules to the electrode surface.

These results demonstrate functionality of the biosensor in more complex cell culture media with good reproducibility and linearity range and highlight the need to perform appropriate calibration in the specific media for ensuring accurate quantification of $O_2^{\bullet-}$ in biological environments. The limit of detection (LOD) of the biosensor was calculated according to the $3\sigma/R$ criteria, where R is the slope of the linear calibration curve in terms of square root of XOD concentration and σ is the standard deviation of the amperometric signal from the blank buffer [38]. The LODs of the biosensor were 86.21 nM in 0.1 M PBS buffer and 9.9 nM in cell culture. To further confirm the biosensor specificity and demonstrate that the signal was due to $O_2^{\bullet-}$ release, we added SOD, which is known to catalyze the dismutation of $O_2^{\bullet-}$. A significant increase of the signal was observed after SOD (10 U/mL) addition, stabilizing at a value close to the background current. These results demonstrate that the released $O_2^{\bullet-}$ was effectively inactivated by the SOD and the signal was indeed associated with $O_2^{\bullet-}$, confirming specificity of measurements.

The optimized biosensor was further tested to establish stability and reproducibility of measurements. The biosensor was stored in 0.1 M PBS at 4 °C when not in use. The sensor's response decreased in the first day, but then it stabilized for the following 7 days (Figure S2). The biosensor showed a good reproducibility, with all measurements reported for at least 3 independently prepared electrodes, with an average standard deviation of the signal consistently below 8%. We note however that when used for measurements, the biosensors will require calibration in the testing environment. The detection sensitivity of this method is comparable with other types of SOD-based biosensors reported in the literature for cell culture measurements (Table S2).

Biosensor selectivity

To further confirm selectivity of measurements and evaluate the use of the biosensor in cell cultures, we conducted amperometric measurements at − 0.2 V and measured the signal generated with the addition of interfering molecules including 3,4-dihydroxyphenylacetic acid (DOPAC, 10 µM),

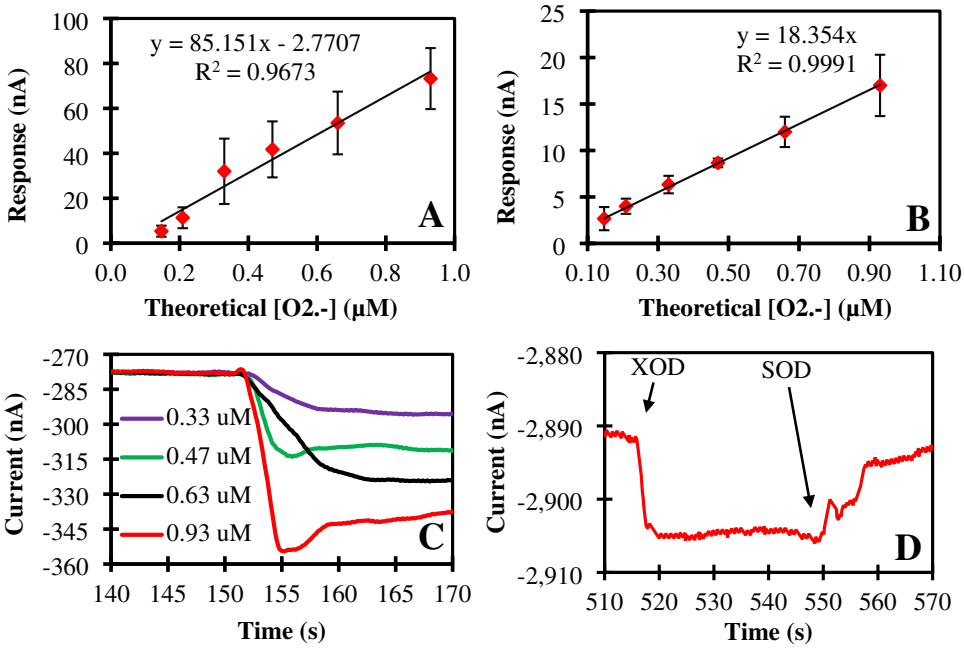

Fig. 4 Calibration of the fabricated biosensor obtained in 0.1 M PBS at pH 7.5 (**A**), cell culture medium (**B**). Error bars indicate the mean of $n = 4$ independent experiments respectively and the standard deviation. The amperograms recorded for various concentrations of $O_2^{\bullet-}$ generated by addition of HX (**C**). The specificity of sensor towards $O_2^{\bullet-}$ upon addition of SOD enzyme to suppress the enzymatically generated $O_2.^{\bullet-}$radicals leading to decrease signal (increase in current values) (**D**). All experiments were performed with $n = 4$ independently prepared electrodes and potential is versus Ag/AgCl (1 M)

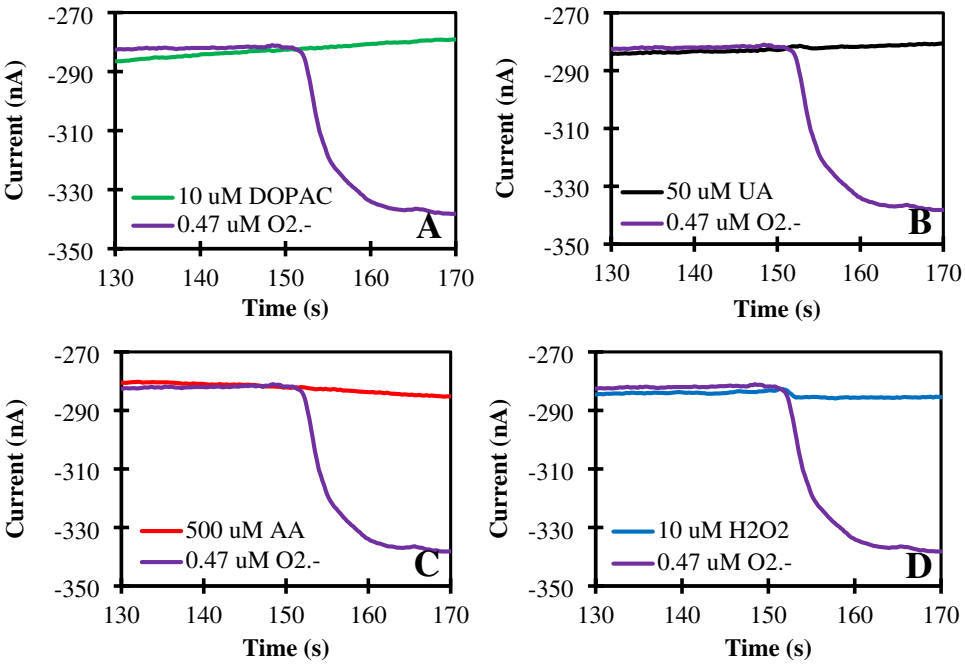

Fig. 5 Sensor response to 10 µM DOPAC (**A**), 50 µM UA (**B**), 500 µM AA (**C**), or 10 µM H_2O_2 (**D**) measured in 0.1 M PBS, pH 7.5

uric acid (UA, 50 µM), ascorbic acid (AA, 500 µM), and H_2O_2 (10 µM). Ascorbic acid and uric acid are commonly found in biological systems at relatively high concentrations and are known to cause interferences due to their electroactive character and low oxidation potentials [36]. DOPAC is a metabolite of dopamine and is similarly ubiquitous in biological systems [39]. H_2O_2 is produced in the degradation of $O_2^{\bullet-}$ and is a byproduct in the enzymatic reaction between HX and XOD that was used to calibrate the sensor, and therefore an important interferent in SOD-based $O_2^{\bullet-}$ sensors [12]. The data, summarized in Fig. 5A–D, indicate no significant response from the interferences tested showing that the biosensor is selective for $O_2^{\bullet-}$. The optimized biosensor was further used to quantitatively measure $O_2^{\bullet-}$ released by THP-1 cells under normal and stimulated conditions.

Superoxide measurements in THP-1 cell line

To evaluate the ability of the developed probe to detect $O_2^{\bullet-}$ of cellular origin, human leukemia monocytic THP-1 cells were stimulated with 2 µg/mL lipopolysaccharide (LPS) and current response of the sensor was recorded continuously over a period of 10 h. LPS is found within the cell wall of Gram-negative bacteria. It can stimulate

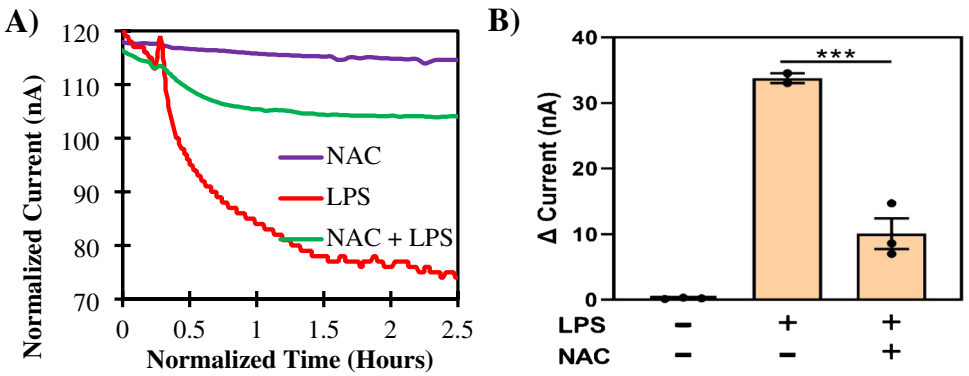

Fig. 6 **A** Amperometric recordings showing the normalized current signal of the sensor in THP-1 cells with and without stimulation of LPS. Measurements were conducted over a period of 10 h; the current and time scales shown are normalized to show the changes in a single figure (original raw data are provided in SI). **B** The quantified signal is represented as a bar graph with each dot representing the individual data point collected. The control is zero as there was no addition of LPS and hence no change in current. Error bars indicate the mean ± standard deviation of three independent measurements

cells via toll-like receptors, triggering a pro-inflammatory response and therefore inducing the production of ROS [40, 41]. The signal of the $O_2^{\bullet-}$ probe increased rapidly upon LPS stimulation when compared with that of untreated cells (Fig. 6). Furthermore, the LPS-induced $O_2^{\bullet-}$ signal was significantly reduced for the cells pretreated with 15 mM N-acetyl L-cysteine (NAC), which is a widely used antioxidant that functions by triggering cell responses rather than by acting as a scavenger itself [42]. Although LPS also induces the expression of inducible nitric oxide synthase (iNOS) to produce nitric oxide (NO), another member of ROS superfamily, it generally takes more than 2 h for LPS-induced expression of iNOS [43].

This sensor has additionally shown specificity for $O_2^{\bullet-}$ ions. Therefore, it can be concluded that there was little to no NO released from the LPS-stimulated cells in the early-stage stimulation and the signal was mainly contributed by $O_2^{\bullet-}$. The raw data showing the amperometric responses monitored over 10 h for the (i) control cells pre-incubated in NAC without addition of LPS, (ii) cells where just LPS has been added, and (iii) cells pre-incubated in NAC with the addition of LPS are shown in Figure S3 in SI, without the normalization. These results indicate that the developed probe could monitor the extracellular $O_2^{\bullet-}$ for the control (~ 1.86 μM) and that of the cells pre-incubated with LPS (0.55 μM) which was roughly a threefold decrease.

Conclusions

In summary, this study demonstrated an electrochemical biosensor platform that provides an easy and convenient way to measure cellular $O_2^{\bullet-}$ release that can be broadly applicable to study oxidative stress and related mechanisms in biological environments. Fundamentally, the study demonstrates significant enhancement of the biosensor response provided by the synergistic contribution of a biohybrid system combining a biological $O_2^{\bullet-}$ specific enzyme with a high surface area redox catalyst, $Ti_3C_2T_x$ MXenes, as an electrode material and catalytic amplifier. The low detection potential removed potentially interfering signals from co-occurring species commonly found in biological environments, imparting selectivity, and demonstrated good functionality in complex cellular systems. This new design enabled real-time quantitative detection of $O_2^{\bullet-}$ release and modulation of oxidative stress in THP-1 cell line under normal and stimulated conditions. This electroanalytical tool can be used in future work to study the complex oxidative stress–related mechanisms and advance our knowledge of the relationship between oxidative stress and therapeutic interventions.

Supplementary Information The online version contains supplementary material available at https://doi.org/10.1007/s00216-024-05437-z.

Acknowledgements We acknowledge funding from US-National Science Foundation grant (NSF 20425544) to SA. Any opinions, findings, and conclusions or recommendations expressed in this material are those of the author(s) and do not necessarily reflect the views of the National Science Foundation. The authors would also like to acknowledge Dr. Daniel Andreescu, Hubert Bilan and Center for Advanced Material Processing (CAMP), for assistance with material characterization and the usage of SEM facility. Tyler Bechard would like to acknowledge the Clarkson Honors program for the research opportunity provided. K.L. acknowledges the support from NIH grants (R35GM147112 and R35GM147112-02S2).

Author contribution Aaditya Deshpande: conceptualization, methodology, analysis, investigation, writing—original draft; Tyler Bechard: analysis, investigation (bioelectrode); Emily DeVoe: analysis, investigation (bioelectrode); Jared Morse: analysis, investigation (cell cultures); Reem Khan: analysis, investigation (MXenes), Ka Ho Leung—resources, funding acquisition, review and editing; Silvana Andreescu—conceptualization, resources, project administration, funding acquisition, review and editing.

Declarations

Competing interests The authors declare no competing interests.

References

1. Klaunig JE, Kamendulis LM, Hocevar BA. Oxidative stress and oxidative damage in carcinogenesis. Toxicol Pathol. 2010;38(1):96–109.
2. Jomova K, Vondrakova D, Lawson M, Valko M. Metals, oxidative stress and neurodegenerative disorders. Mol Cell Biochem. 2010;345(1):91–104.
3. Krumova K, Cosa G. Chapter 1 Overview of reactive oxygen species. Singlet oxygen: applications in biosciences and nanosciences, Volume 1. 1: The Royal Society of Chemistry; 2016. pp. 1–21.
4. Wang Y, Branicky R, Noë A, Hekimi S. Superoxide dismutases: dual roles in controlling ROS damage and regulating ROS signaling. J Cell Biol. 2018;217(6):1915–28.
5. Prasad A, Balukova A, Pospisil P. Triplet excited carbonyls and singlet oxygen formation during oxidative radical reaction in skin. Front Physiol. 2018;9:1109.
6. Togashi H, Aoyama M, Oikawa K. Imaging of reactive oxygen species generated in vivo. Magn Reson Med. 2016;75(3):1375–9.
7. Mao GD, Poznansky MJ. Electron spin resonance study on the permeability of superoxide radicals in lipid bilayers and biological membranes. FEBS Lett. 1992;305(3):233–6.
8. Wang HS. Development of fluorescent and luminescent probes for reactive oxygen species. Trac-Trend Anal Chem. 2016;85:181–202.
9. Ohyashiki T, Nunomura M, Katoh T. Detection of superoxide anion radical in phospholipid liposomal membrane by fluorescence quenching method using 1,3-diphenylisobenzofuran. Biochimica et Biophysica Acta (BBA) - Biomembranes. 1999;1421(1):131–9.
10. Ohara Y, Peterson TE, Harrison DG. Hypercholesterolemia increases endothelial superoxide anion production. J Clin Investig. 1993;91(6):2546–51.

11. Rojas D, Hernandez-Rodriguez JF, Della Pelle F, Escarpa A, Compagnone D. New trends in enzyme-free electrochemical sensing of ROS/RNS. Application to live cell analysis. Mikrochimica acta. 2022;189(3):102.
12. Calas-Blanchard C, Catanante G, Noguer T. Electrochemical sensor and biosensor strategies for ROS/RNS detection in biological systems. Electroanalysis. 2014;26(6):1277–86.
13. Deshpande AS, Muraoka W, Wait J, Colak A, Andreescu S. Direct real-time measurements of superoxide release from skeletal muscles in rat limbs and human blood platelets using an implantable cytochrome C microbiosensor. Biosens Bioelectron. 2023;240: 115664.
14. Ganesana M, Erlichman JS, Andreescu S. Real-time monitoring of superoxide accumulation and antioxidant activity in a brain slice model using an electrochemical cytochrome c biosensor. Free Radical Biol Med. 2012;53(12):2240–9.
15. Liu X, Marrakchi M, Jahne M, Rogers S, Andreescu S. Real-time investigation of antibiotics-induced oxidative stress and superoxide release in bacteria using an electrochemical biosensor. Free Radical Biol Med. 2016;91:25–33.
16. Fridovich I. Superoxide dismutases. Adv Enzymol Relat Areas Mol Biol. 1974;41:35–97.
17. Saltzman HA, Fridovich I. Oxygen toxicity Introduction to a protective enzyme: superoxide dismutase. Circulation. 1973;48(5):921–3.
18. Morris DR, Koffron KL. Putrescine biosynthesis in Escherichia coli. J Biol Chem. 1969;244(22):6094–9.
19. Fridovich I. The biology of oxygen radicals. Science. 1978;201(4359):875–80.
20. Youn H-D, Kim E-J, Roe J-H, Hah YC, Kang S-O. A novel nickel-containing superoxide dismutase from Streptomyces spp. Biochem J. 1996;318:889–96.
21. Fridovich I. Oxygen toxicity: a radical explanation. J Exp Biol. 1998;201:1203–9.
22. Ohsaka T, Tian Y, Shioda M, Kasahara S, Okajima T. A superoxide dismutase-modified electrode that detects superoxide ion. Chem Commun. 2002;9:990–1.
23. Beissenhirtz MK, Scheller FW, Viezzoli MS, Lisdat F. Engineered superoxide dismutase monomers for superoxide biosensor applications. Anal Chem. 2005;78(3):928–35.
24. Di J, Bi S, Zhang M. Third-generation superoxide anion sensor based on superoxide dismutase directly immobilized by sol–gel thin film on gold electrode. Biosens Bioelectron. 2004;19(11):1479–86.
25. Tian Y, Mao L, Okajima T, Ohsaka T. A carbon fiber microelectrode-based third-generation biosensor for superoxide anion. Biosens Bioelectron. 2005;21(4):557–64.
26. Tian Y, Shioda M, Kasahara S, Okajima T, Mao L, Hisabori T, et al. A facilitated electron transfer of copper–zinc superoxide dismutase (SOD) based on a cysteine-bridged SOD electrode. Biochim Biophys Acta. 2002;1569(1–3):151–8.
27. Naguib M, Mashtalir O, Carle J, Presser V, Lu J, Hultman L, et al. Two-dimensional transition metal carbides. ACS Nano. 2012;6(2):1322–31.
28. Anasori B, Lukatskaya MR, Gogotsi Y. 2D metal carbides and nitrides (MXenes) for energy storage. Nat Rev Mater. 2017;2(2):16098.
29. Kim H, Alshareef HN. MXetronics: MXene-enabled electronic and photonic devices. ACS Materials Letters. 2020;2(1):55–70.
30. Khan R, Andreescu S. MXenes-based bioanalytical sensors: design, characterization, and applications. Sensors [Internet]. 2020;20(18):5434.
31. Wang F, Yang CH, Duan CY, Xiao D, Tang Y, Zhu JF. An organ-like titanium carbide material (MXene) with multilayer structure encapsulating hemoglobin for a mediator-free biosensor. J Electrochem Soc. 2015;162(1):B16-B21.
32. Lorencova L, Bertok T, Dosekova E, Holazova A, Paprckova D, Vikartovska A, et al. Electrochemical performance of Ti(3)C(2)T(x) MXene in aqueous media: towards ultrasensitive H2O2 sensing. Electrochim Acta. 2017;235:471–9.
33. Alhabeb M, Maleski K, Anasori B, Lelyukh P, Clark L, Sin S, et al. Guidelines for synthesis and processing of two-dimensional titanium carbide (Ti3C2Tx MXene). Chem Mater. 2017;29(18):7633–44.
34. Vreeland RF, Atcherley CW, Russell WS, Xie JY, Lu D, Laude ND, et al. Biocompatible PEDOT: Nafion composite electrode coatings for selective detection of neurotransmitters in vivo. Anal Chem. 2015;87(5):2600–7.
35. Özel RE, Alkasir RSJ, Kayla R, Wallace KN, Andreescu S. Comparative evaluation of intestinal nitric oxide in embryonic zebrafish exposed to metal oxide nanoparticles. Small. 2013;9(24):4250–61.
36. Tian Y, Mao L, Okajima T, Ohsaka T. Superoxide dismutase-based third-generation biosensor for superoxide anion. Anal Chem. 2002;74(10):2428–34.
37. Nagarajan RD, Sundaramurthy A, Sundramoorthy AK. Synthesis and characterization of MXene (Ti(3)C(2)T(x))/iron oxide composite for ultrasensitive electrochemical detection of hydrogen peroxide. Chemosphere. 2022;286(Pt 1): 131478.
38. Currell G. Analytical instrumentation: performance characteristics and quality. New York: John Wiley & Sons; 2008.
39. Fuller RW, Perry KW. Effect of lergotrile on3,4-dihydroxyphenylacetic acid (DOPAC) concentration and dopamine turnover in rat brain. J Neural Transm. 1978;42(1):23–35.
40. Hsu H-Y, Wen M-H. Lipopolysaccharide-mediated reactive oxygen species and signal transduction in the regulation of interleukin-1 gene expression*. J Biol Chem. 2002;277(25):22131–9.
41. Obeng E, Ding F, He X, Shen J. Bioimaging of superoxide anions in living cells and in vivo: perfect visualization with fluorescence probes and their applications. Dyes Pigm. 2022;199: 109964.
42. Ezeriņa D, Takano Y, Hanaoka K, Urano Y, Dick TP. N-acetyl cysteine functions as a fast-acting antioxidant by triggering intracellular H2S and sulfane sulfur production. Cell Chemical Biology. 2018;25(4):447-59.e4.
43. Hwang J-SK, Kwon MY, Kim KH, Lee Y, Lyoo IK, Kim JI, Oh ES, Han IO. Lipopolysaccharide (LPS)-stimulated iNOS induction is increased by glucosamine under normal glucose conditions but is inhibited by glucosamine under high glucose conditions in macrophage cells. J Biol Chem. 2017;3;292(5):1724–36.

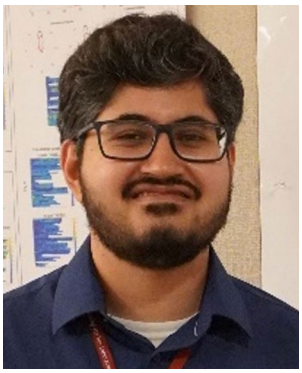

Aaditya S. Deshpande received his Ph.D. in chemistry from Clarkson University under the supervision of Prof. Silvana Andreescu. He is currently a postdoc at the University of Virginia in Dr. Jill Venton's group. He has worked on the design, fabrication, and surface characterization of biosensors for monitoring biomarkers in zebrafish embryos, rat limbs, cell lines, and plant assays. His current work involves the measurement of neurotransmitters in *Drosophila melanogaster* brain using electrochemical techniques and fluorescence microscopy.

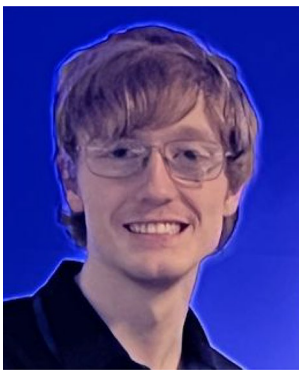

Tyler Bechard completed his BS in chemistry as an honor student at Clarkson University, where he conducted research on the development of enzymatic biosensors for monitoring oxidative stress in the laboratory of Prof. Silvana Andreescu. He is continuing his education as a graduate student at the University of Illinois at Urbana Champaign.

Emily DeVoe graduated from SUNY Potsdam in 2021 with honors in analytical chemistry. She is currently a chemistry graduate student in the Department of Chemistry and Biochemistry at Clarkson University, where she performs research with a focus on implantable enzymatic biosensors for real-time monitoring of dopamine and other neurotransmitters using in-lab fabricated carbon fiber microelectrodes.

Jared Morse is currently a PhD candidate in the Department of Chemistry and Biochemistry at Clarkson University in Prof. Ka Ho Leung's group. His research interest lies in the field of chemical biology, particularly on how intracellular ion homeostasis regulates critical cellular processes and relates to health and disease.

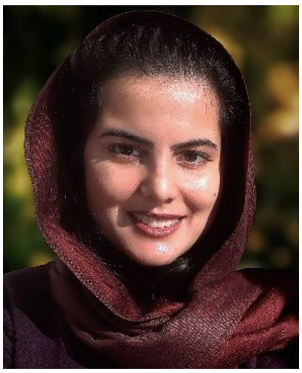

Reem Khan received her Ph.D. from Clarkson University working with Prof. Silvana Andreescu and is currently a postdoctoral research fellow at Carnegie Mellon University. Her research focuses on exploring various materials for sensing and biosensing applications, with specific interests in implantable biosensors and the sensing of environmental contaminants.

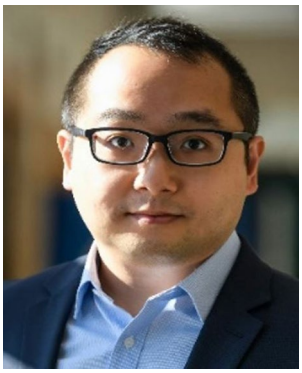

Ka Ho Leung joined Clarkson University, USA, as Assistant Professor in the Department of Chemistry & Biomolecular Science in 2021. His research focuses on designing innovative imaging tools capable of quantifying chloride and related chemicals within various specific cellular organelles, and leveraging these developed tools to deconvolute the physiological role of chloride.

Silvana Andreescu is currently Chair of Environmental Health Sciences at Florida International University (FIU). Previously, she was Professor and Egon Matijevic Chair in the Department of Chemistry and Biomolecular Science at Clarkson University. Her research program integrates electroanalytical, biochemical, and materials science advances to develop innovative sensing technology for human and environmental health. Her recent work features the development of real-time chemical and biological sensors for real-time monitoring of disease biomarkers, oxidative stress, neurochemicals, and environmental contaminants in clinical and environmental samples.